Heat transfer phenomena during processing materials with microwave energy

Domenico Acierno, Anna Angela Barba,

Matteo d'Amore

Abstract This paper analyses transport phenomena that occur during microwave heating. In particular, a transient one-dimensional energy balance equation has been adopted to describe the heating of a body in a microwave cavity (single-mode applicator). In the energy balance, a kinetic term has been introduced to take into account released or absorbed heat due to chemical reaction. Thus, the energy equation has been coupled with a mass balance and the relevant initial and boundary conditions. Modeled heating profiles are shown to describe the energy transfer in different materials and, the influence, on the heating process, of the fluid-dynamics outside the microwave cavity is studied and discussed.

1
Introduction

Microwave energy is an innovative tool for heating processes, although microwaves have been firstly adopted for communications scope. Reasons for the growing interest to microwave heating applications can be found in benefits such as reductions in manufacturing costs due to energy saving and shorter processing times, improved product uniformity and yields, improved or unique microstructure and properties, and, synthesis of new materials [1].

These advantages have focused the attention on the use of electromagnetics in many applications: from the materials processing, with special reference to food [2], polymers (curing), wood, ceramics and composites [3]–[5]; to minerals treatments [6], [7], and environmental remediation processes (soil remediation, toxic waste inertization) [8], [9].

D. Acierno
Dept. of Materials and Production Engineering,
University of Naples "Federico II", Piazzale Tecchio 80,
80125 Napoli, Italy

A. A. Barba (✉), M. d'Amore
Dept. of Chemical and Food Engineering,
University of Salerno Via Ponte Don Melillo, 84084 Fisciano, Italy
E-mail: aabarba@unisa.it
Tel.: +39 089964026
Fax: +39 089964057

1.1
Microwave heating

The peculiarity of the microwave heating is the energy transfer. In conventional heating processes, energy is transferred to the material by convection, conduction and radiation phenomena through the external materials surface, in presence of thermal gradients. In contrast, microwave energy is delivered directly to materials through molecular interactions with electromagnetic field via conversions of electromagnetic energy into thermal energy [3].

The ability of a material to interact with electromagnetic energy is related to the material's complex permittivity. This property, usually indicated with the Greek symbol ε, is expressed by the real part, ε', or *dielectric constant* and the imaginary part, ε'', or *loss factor*. The dielectric constant is a measure of how much energy from an external electric field is stored in the material; the loss factor accounts for the loss energy dissipative mechanisms in the material. Therefore, a material with a high loss factor is easily heated by microwave. Knowledge of the complex permittivity is fundamental for material processing, because it has a strong influence on the choice of microwave devices and the set-up of working protocols.

1.2
Microwave devices

The applicator is a device that provides a means for applying the microwave energy from the generator to the workload (material to be heated). How to supply microwave energy depending on the electromagnetic field distribution in the applicator induced by the resonant *modes* (solutions of the Maxwell equations coupled with suitable boundary conditions).

Typical microwave applicators are, travelling wave guides, single-mode and multi-mode cavities (or ovens).

Multi-mode ovens are the most commonly used form of microwave heating applicator (e.g. domestic microwave ovens). The denomination is due to their ability of sustaining many modes related to the dimensions of cavities. In particular, as the size of the microwave cavity increases, the number of possible resonant modes increases. From a mechanical point of view, they are very simple, essentially consisting of a closed metal box with accessories, being thus easy to realize. The popularity of the multimode ovens arises not only from their mechanically simplicity but also from their ability to process a very wide range of workloads different in size and dielectric properties. However, the simplicity ends here, since the

electromagnetic analysis is extremely complicated, being the field pattern the results of a large number of simultaneous resonant modes. Moreover, the presence of different modes generates in multiple hot spots, due to very different spatial field strength within the cavities. Nevertheless, to improve the field uniformity, several efficient systems are used (workload traveling, mode stirred, hybrid heating -dielectric and conventional heat transfer coupled-).

Single-mode cavities support only one mode at the source frequency, so that the field pattern is well defined in space [10], [12]. Since the electromagnetic field can be determined using analytic or numerical techniques, the areas of high and low electromagnetic field are known. This is useful for many purposes, especially in laboratory-scale studies, for example to monitor dielectric properties during investigation of microwave/materials interactions. In general, single-mode cavities have only one hot spot where the microwave field strength is high, and usually the area of high energy intensity is confined. Then, single-mode applicators are used every time is important to focus microwave energy (e.g. joint applications of ceramics, melting of multi-phase low-loss/high loss materials, selective heating of little areas of material to start a chemical reaction); to heat filamentary materials, to cure polymers [3], [9], which are weak absorbers of microwaves.

Aim of this work is to simulate heating processes of weak and weak "activated" microwave absorbers (workloads) in a single-mode applicator, in presence and without chemical reactions, under different external fluid-dynamics conditions.

2
Model outline

2.1
Generalized balance equations
The generalized energy balance code written to numerically solve heating balance equations has been already described in a previous paper [13] which also reports a preliminary validation performed by comparing the results of the code with several analytical solutions obtained from the literature. In the following, the generalized form of energy balance is briefly summarized and the corresponding mass balance is proposed, together with the coupling terms, i.e. kinetic rate function and latent heat:

$$\frac{\partial T(t,\xi)}{\partial t} = \alpha_T \left(\frac{f}{\xi}\frac{\partial T(t,\xi)}{\partial \xi} + \frac{\partial^2 T(t,\xi)}{\partial \xi^2} \right) + \frac{\alpha_T G(t,\xi)}{k} \quad (1)$$

$$G(t,\xi) = \sum_{j=1}^{M} \dot{Q}_{gj}(t,\xi) + \sum_{i=1}^{N} r_i(t,\xi)\Delta H_i \quad (2)$$

In Eq. (1), t and ξ are the time and space variables respectively; $T(t,\xi)$ is the temperature; material parameters are thermal diffusivity α_T and thermal conductivity k. Eq. (2) also accounts for M different heat source terms $\dot{Q}_{gj}(t,\xi)$ and for N different latent release/absorption heats due to chemical reaction or phase change $r_i(t,\xi)\Delta H_i$. Flag f

can be 0, 1 or 2, describing the heat transfer problem in a semi-infinite flat slab ($\xi \equiv z$ = axial direction), in a semi-infinite cylinder ($\xi \equiv r$ = radial direction) or in a sphere ($\xi \equiv r$ = radial direction) respectively. Eq. (1) can be coupled with N different mass balance equation for the N different species:

$$a_i \frac{\partial C_i(t,\xi)}{\partial t} = r_i(t,\xi) \quad \forall i - 1,\ldots,N \quad (3)$$

where $C_i(t,\xi)$ are the chemical species concentrations and a_i are parameters accounting for density, porosity and dimensions adopted for C_i. Functions $r_i(t,\xi)$, already reported in Eq. (2), are kinetic rates. Model is completed by suitable initial and boundary conditions. Standard form of initial conditions is:

$$\text{I.C.} \quad @t=0 \quad \begin{cases} T(0,\xi) = T_0(\xi) \\ C_i(0,\xi) = C_{0i}(\xi) \end{cases} \quad (4)$$

Boundary conditions can be written in a generalized form ($n = 1, 2$):

$$\text{B.C.} \quad @\xi = \Xi_n \quad \alpha_n(t)\left.\frac{\partial T}{\partial \xi}\right|_{\xi=\Xi_n} + \beta_n(t)T|_{\xi=\Xi_n} + \gamma_n(t) = 0$$
$$(5)$$

in Eq. (5) $\alpha_n(t)$, $\beta_n(t)$ and $\gamma_n(t)$ are parameters useful to reproduce usual forms of boundary conditions. A detailed description of the values the coefficients assume in different cases is reported in [13].

2.2
Applied model equations
In this work induced microwave heating of cylindrical workloads, using a single-mode cylindrical applicator is studied. Due to the loads geometry, in the generalized balance Eq. (1) the shape flag is $f = 1$, and space variable ξ is the radial direction, bounded by the cavity radius b. Thus, for the modeling purposes, our system consists in an irradiated material with a radius equal to the cavity radius b, enclosed in a thin metallic shell (the cavity itself). The Eq. (1) is enough to describe the process because for a long cylinder, on the basis of an order of magnitude reasoning, the axial conduction phenomenon can be neglected, if compared with radial conduction. Having in mind the system to heat above described, the structure of the generalized Eq. (5) becomes:

$$\text{B.C.1} \quad @\xi = 0; \quad \forall t>0 \quad \left.\frac{\partial T}{\partial \xi}\right|_{\xi=0} = 0 \quad (6)$$

$$\text{B.C.2} \quad @\xi = b; \quad \forall t>0 \quad k\frac{\partial T}{\partial \xi} = -U(T - T_\infty) \quad (7)$$

where k is the thermal conductivity and T_∞ is the bulk temperature and U is the overall heat exchange coefficient. This latter has in account for heat exchanges by conduction in metallic shell (cavity wall), by convection and radiation in the surrounding. Neglecting the conduction phenomenon due to the high conductivity and low thickness of the metallic wall, the heat exchange coefficient, for

free convection from horizontal tubes plus radiating losses, can be evaluated by [14]:

$$U(T) \cong h(T)$$
$$= \left[1.32 \cdot (T - T_\infty)^{1/4} \cdot (2b)^{-1/4} \right]$$
$$+ \left[\sigma \cdot \varepsilon_{irr} \cdot \frac{(T^4 - T_\infty^4)}{(T - T_\infty)} \right] \tag{8}$$

where σ and ε_{irr} are the Stefan-Boltzmann's and the emissivity constants, respectively. Values of code parameters are reported in Table 1.

2.3
Heat generation by microwave and by chemical reaction

For this study a 2.45 GHz in frequency and 900 W in power microwave source (magnetron) is supposed to be connected to a closed cylindrical cavity. This latter is characterized to have the critical dimension, the diameter, able to support the TM_{010} (Transverse Magnetic mode, i.e. the magnetic field propagating does not have an axial component) resonance mode. Cylindrical cavity operation in TM_{010} mode is commonly preferred, because of the electromagnetic distribution in such a cavity. The propagation of TM_{010} mode descends from the cavity diameter which, in turn, is function of the dielectric properties as explained in the following.

Thus, only one heat source term ($M = 1$) is considered in the Eq. (1) and it is described by the common form of the average power loss density drawn from the Poynting's theorem [10], [12]:

$$\dot{Q}_g(t, \xi) = \frac{1}{2} \omega \varepsilon_0 \varepsilon''(t, \xi) |E(\xi)|^2 \tag{9}$$

where ω is the angular frequency, ε_0 is the vacuum permittivity, ε'' is the material loss factor and E is the field strength. In TM_{010} single-mode cylindrical cavity the electric field strength is described by Eq. (10):

$$E(\xi) = 0 \cdot \underline{i}_r + 0 \cdot \underline{i}_\phi + E_{max} J_0 \left(\frac{x_{01}}{b} \xi \right) \cdot \underline{i}_z \tag{10}$$

where E_{max} is the maximum field strength, x_{01} is the first root of the J_0 the 0-th Bessel function of first kind, b, as above reported, is the radius of the cylindrical closed cavity, and $\underline{i}_r$, $\underline{i}_\phi$, $\underline{i}_z$ are the unit vectors for the adopted reference system. Figure 1 reports the dimensionless electrical field strength ($E(\xi)/E_{max}$) in a single mode cavity as a function of the dimensionless cavity radius (ξ/b). It is worth noticing that the electric field is not dependent upon axial coordinate. As consequence, for a cylinder with well insulated basis surfaces (regardless from its L/D – length/diameter ratio-value) there is no reasons for inducing an axial temperature gradient. This is a further confirmation for disregard the axial heat conduction term.

Table 1. Values of code parameters

f	Ξ_1	α_1	β_1	γ_1	Ξ_2	α_2	β_2	γ_2
1	0	1	0	0	b	k	h	$-hT_\infty$

For materials whose do not exhibit magnetic polarization [10] suggests to calculate the radius cavity, under the condition of filled cavity, adopting the following equation:

$$b = \frac{c}{\omega} \cdot \frac{x_{01}}{\sqrt{|\varepsilon|}} \tag{11}$$

where c is the light velocity and $|\varepsilon|$ is the material permittivity modulus. A cavity built with this radius and completely filled with that material, will sustain only the TM_{010} mode.

To keep the sustainment of the TM_{010} mode the variation of $|\varepsilon|$ must be limited during the treatments. Changes in ε'' that do not strongly affect $|\varepsilon|$ (i.e. if $\varepsilon'' \ll \varepsilon'$) can be easily accounted for $\dot{Q}_g$ (Eq. (9)) calculation. Broad range of ceramic materials, especially used as support-structure, show low and constant values of permittivity if their temperature don't reaches a critical values.

As heat generation by chemical reaction, we assume only one kind of reactant species ($N = 1$) with this kinetic rate:

$$r(t, \xi) = K(t, \xi) \cdot [C(t, \xi)]^n \tag{12}$$

where $K(t, \xi)$ is the kinetics constant and n is the reaction order.

The partial differential equations (Eqs. (1)and(3)), with their initial condition (Eq. (4)) and boundary conditions (Eqs. (5)and(6)) are solved by the finite difference method known as Crank-Nicolson scheme, as described by [15].

3
Results and discussion

Three kinds of model results are presented. As reported above, our attention is focused on heat transfer phenomena during microwave treatments of different materials. Thus, the work is organized in the following sub-sections:

i. microwave heating of both weak and "activated" material absorbers without chemical reaction;
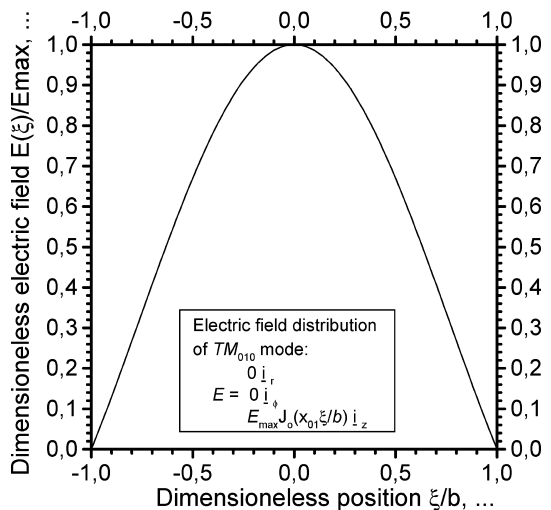ii. microwave heating in presence of chemical reaction;

Fig. 1. Dimensionless electric field radial profile in a TM_{010} single-mode cylindrical cavity

iii. microwave heating under dierent external conditions to investigate the influence of fluid-dynamic parameters on the heat transfer phenomena.

All the model runs are performed using the condition of completely filled cavity. The characteristic parameter of this latter (diameter) is considered as always able to support TM_{010} mode resonance with respect to the dielectrics properties of the material.

In the simulation work, some properties are kept constant, even if in the real treatments they can change. However, their variations do not have not a strong influence on behaviours of real systems.

Finally, each simulation is carried out several times by increasing time and space step numbers, until temperature distributions become independent of the number of these steps.

Physical material characteristics and electromagnetic features are summarized in Table 2 and Table 3.

3.1
Microwave heating without chemical reaction

In this section, microwave heating of two different kinds of materials, weak and "activated" electromagnetic energy absorbers, is described using the above reported equations.

In the Figures 2–5, thermal profiles are reported as a function of exposure time, at two radial coordinates, and as a function of the dimensionless radius, parametric in the time evolution.

The first profiles (Figure 2 and Figure 3) represent the temperature distributions in microwave "transparent" materials (with a low loss factor) usually adopted as catalyst support (ceramics before their "critical" temperature of the thermal runaway, carbonates and silicates), reaction medium, seals (Teflon, insulating such as polymer, wool quartz and glasses) [5], [6]. Their general features are reported in Table 2. Weak microwave absorbers are also basic components of composites which are "activated" by

microwave energy when they are added with strong-loss materials (additives or fillers or active phases) such as carbonaceous and so called "hyperactive" structures: UO_2, SiC, sulphide and oxides iron compounds etc. [6]. Multiphase systems are adopted in microwave assisted sintering of ceramics and glasses and microwave curing of polymers.

In weak absorbers, microwave energy weakly interacts with the material's structure, then the heating process is not very strong and not very fast (Figure 2). Instead, at the same radiating and external fluid-dynamic conditions, in presence of added absorbed microwave additives, the heating process becomes faster, i.e. the steady state is rapidly attained (Figure 4) and the reachable temperatures can differ one order of magnitude. Moreover, neglecting the contributes of the absorbed phase on the thermal properties due the very small addition required, it is important to outline the development of thermal gradients inside the processed materials. Indeed, high thermal gradients can cause stresses that can be high enough to fracture the material. This is the most important problem also in microwave treatments, see for example in ceramics sintering due the low thermal conductivity of the materials. Thus, the knowledge of thermal profiles is crucial to the control of heating treatments, which in turn affects the final quality of products. In particular, Figures 3 and 5 report temperature profiles of the two kinds of irradiated materials. The strong absorber kind (Figure 5) shows a very high thermal gradients for its strong interaction with microwave energy and its low ability to dissipate heat by conductivity phenomena.

In Figure 6 are shown the thermal gradients, calculated at the steady state, induced in materials with different loss factor at various electromagnetic field strength distribution. In particular, at E_{max} 10^4 V/m and for a material with loss factor 2, the thermal gradient is about 27 °C/mm, then in a cylindrical shape body with 15 mm in radius (by Eq. (11)) the temperature difference between the axial and

Table 2. Values and units chosen for physical parameters involved in simulations

Parameter	Value	Units	Parameter	Value	Units
α_T	$1\cdot10^{-7}$	$m^2\cdot s^{-1}$	c	3.10^8	$m\cdot s^{-1}$
k_T	1.5	$J\cdot m^{-1}\cdot°C^{-1}\cdot s^{-1}$	ω	$2\pi2.45\cdot10^{+9}$	s^{-1}
$\rho^\star$	0.9	–	ε_0	$8.85\cdot10^{-12}$	$F\cdot m^{-1}$
T_∞	25	°C	ε'	10	–
$\varepsilon_{irr}^{\star\star}$	0.2	–	ε''	0.1–2	–
σ	$5.67\cdot10^{-3}$	$W\cdot m^{-2}\cdot K^{-4}$	b	15.10^{-3}	m
*porosity; **polished metallic surface			E_{max}	10^4	$V\cdot m^{-1}$

Table 3. Values and units chosen for physical parameters involved in simulations

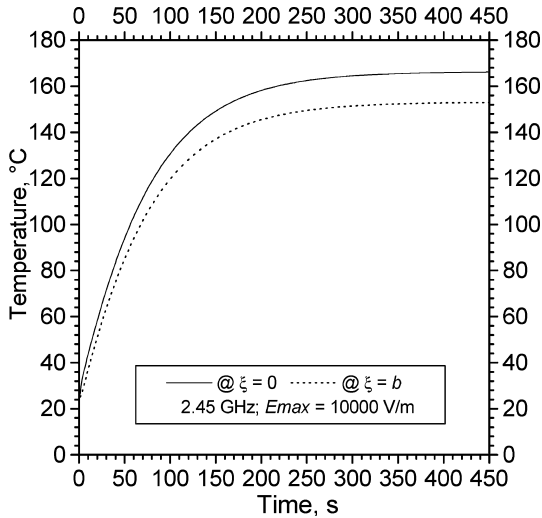| Parameter	Value	Units	Parameter	Value	Units
ΔH	1.10^{-7}	$J\cdot mol^{-1}$	C_0	1.2	% weigh
E_a/R	18000	K	ε_0	$8.85\cdot10^{-12}$	$F\cdot m^{-1}$
R	3.186	$J\cdot mol^{-1}\cdot K^{-1}$	ε'	10	–
K_{c0^*}	$11\cdot10^{-5}$	$g\cdot m^{-3}\cdot s^{-1}$	ε''	2	–
k_Υ	1.5	$J\cdot m^{-1}\cdot K^{-1}\ s^{-1}$	E_{max}	10^4	$V\cdot m^{-1}$
ρ	0.9	–	ω	$2\pi2.45\cdot10^{+9}$	s^{-1}
*Arrhenius' Law: $K_c = K_{c0} \exp\left(-\frac{E_a}{RT}\right)$			b	$15\cdot10^{-3}$	m

Fig. 2. Temperature profiles as a function of the exposure time at two radial coordinate (weak absorber)
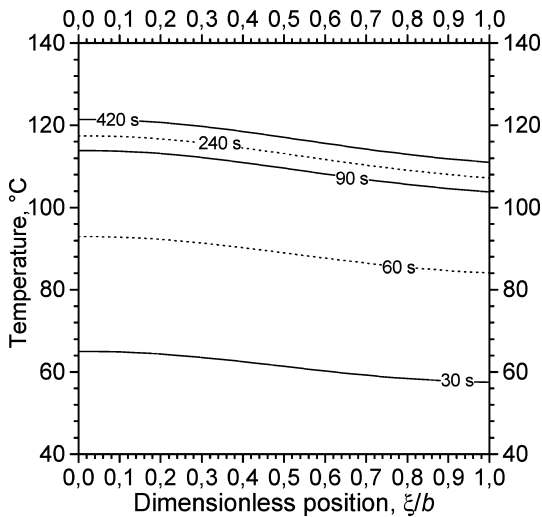

Fig. 3. Temperature profiles as a function of the dimensionless coordinate at different exposure time (weak absorber)
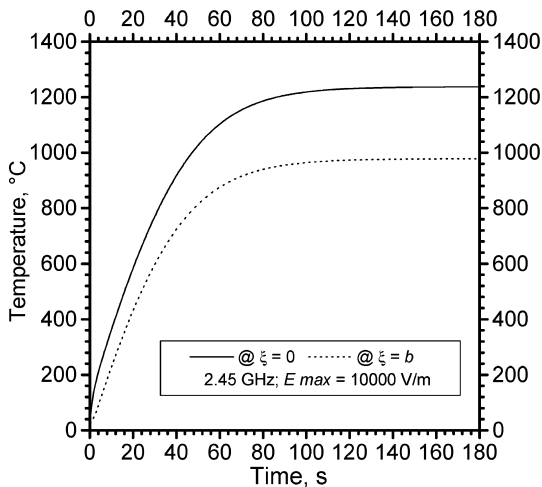

Fig. 4. Temperature profiles as a function of the exposure time at two radial coordinate (activated absorber)
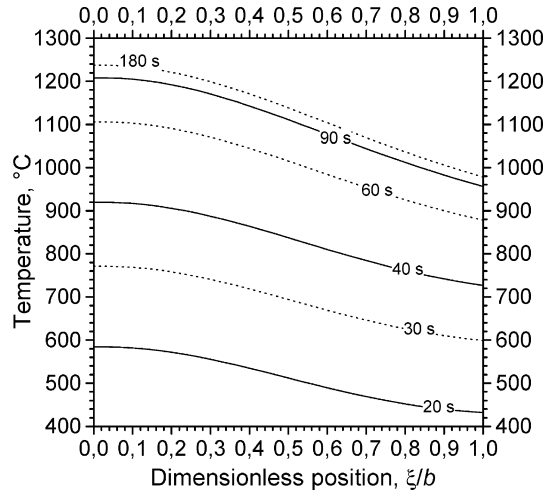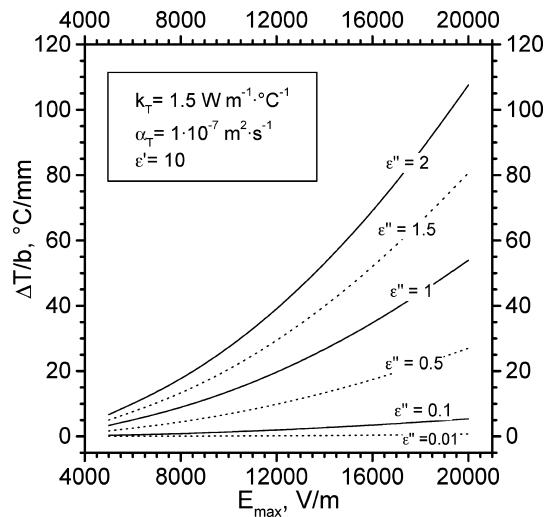

Fig. 5. Temperature profiles as a function of the dimensionless coordinate at different exposure time (activated absorber)

Fig. 6. Thermal gradients (temperature increases per linear unit dimension) at the steady state as function of the maximum fields strength for different loss factor values

the maximum coordinates is larger then 400 °C. Vice versa, in weak absorber ($\varepsilon'' \ll 2$), at the same conditions, lower radial gradients are obtained (in the order of a few degree per mm).

3.2
Microwave heating with chemical reaction
As a model chemical reaction assisted by microwave, we considered an oxidation process. In particular, combustion of carbonaceous-like materials has been simulated (Table 3) using the Arrhenius' law to describe temperature dependence of kinetic constant, and considering the process as a zero order reaction [16], [17]. We supposed that the reaction was carried out in a two-phase system composed by a weak (porous support) and a strong absorbers (carbonaceous-like material). Soot-traps are typical examples of the described system. Their regeneration by microwave-assisted combustion is currently studied [16], [18].

Figure 7 shows the evolution of temperature as a function of time. At the imposed parameters (Table 3), the heating process is very fast, chemical reaction is completed in a few tenths of seconds, as can be seen in Figure 8 where the evolution of chemical reactant concentration with time is reported.

The axial temperature (solid lines in Figures 7 and 9) initially increases at the same heating rate experienced in a pure heating experiment (Figure 2). After about 30 s, ignition temperature is achieved and chemical reaction starts (Figure 8). As a consequence, heating rate increases, then temperature sharply raises and reactant concentration decreases (Figure 10 and 11). When the reactant in the axial zone is over, at the same spatial coordinate, temperature begins to decrease, since no more latent heat is supplied by reaction and the system has become weak in microwave energy dissipation. At the same time, the reaction heat flux moves in radial direction where causes the attainment of the ignition point in outer radial layers together with the heat generated by microwave in the
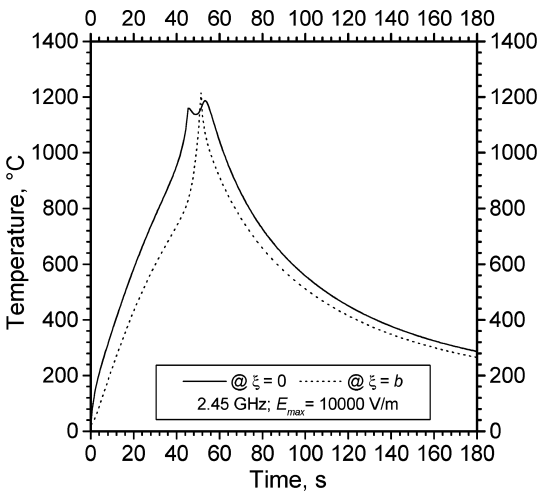

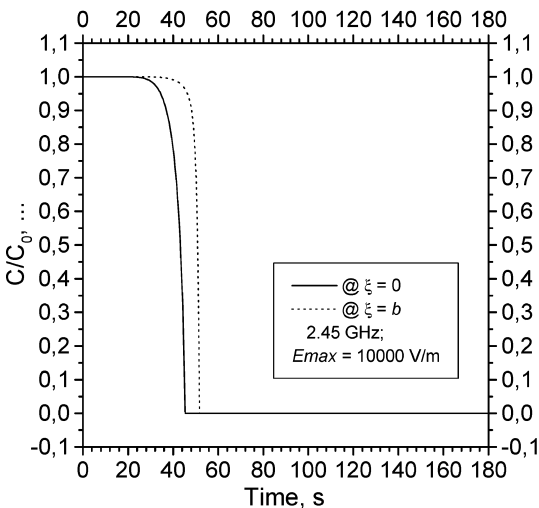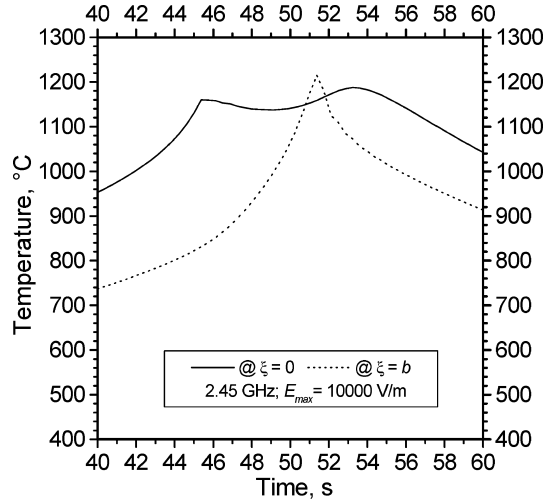**Fig. 9.** Close-up of temperature evolutions as a function of exposure time at two radial coordinates

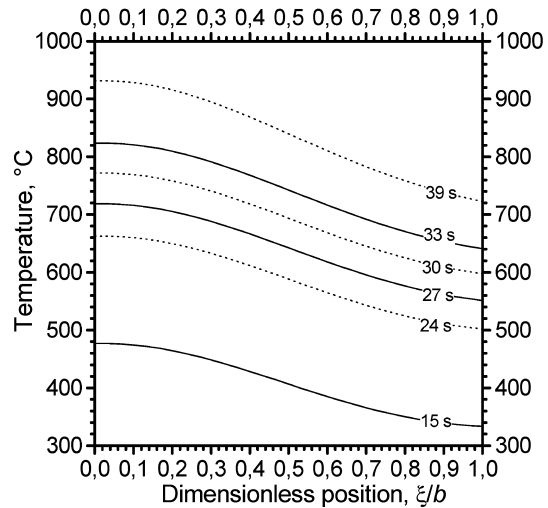**Fig. 7.** Temperature evolutions as a function of exposure time at two radial coordinates

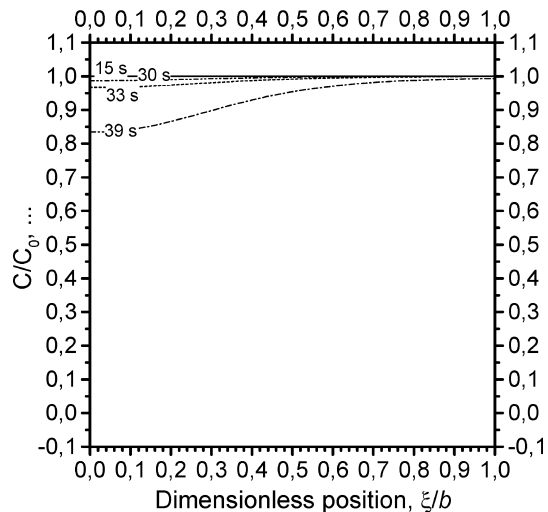**Fig. 10.** Temperature profiles as a function of the radial coordinate at different time

Fig. 8. Reactant concentrations as a function of exposure time at two radial coordinates

Fig. 11. Reactant concentrations as a function of the radial coordinate at different time

Fig. 12. Temperature profiles as a function of the radial coordinate at different time

Fig. 13. Reactant concentrations as a function of the radial coordinate at different time
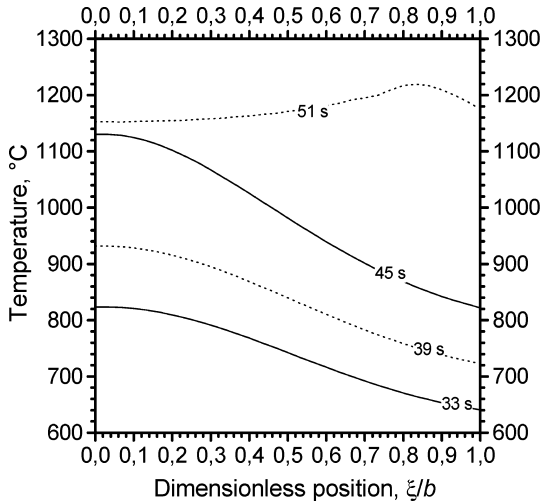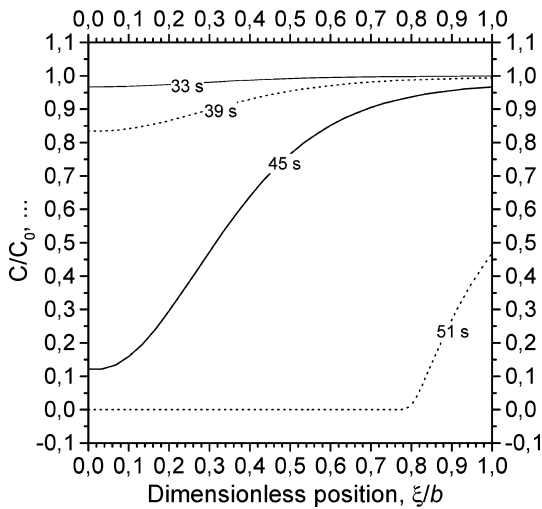

Fig. 14. Temperature evolutions as a function of exposure time at two radial coordinate (at insulated cavity conditions)

Fig. 15. Temperature evolutions as a function of exposure time at two radial coordinate (at first cooling conditions)

unburned sections. By this way, reaction front moves along the radial coordinate (Figure 13) where a maximum in temperature is also achieved (Figure 12). High temperatures reached in outer layers then cause a temporary inversion of radial heat fluxes, and the inner layers are re-heated (dotted line in Figures 7 and 9): the axial temperature shows a new maximum due to the heat coming from boundary regions.

3.3
Microwave heating at different external conditions
In this sub-section, the influence of different external conditions on heat and mass transfer phenomena is examined. As reported in the Model outline, boundary condition 2 takes in to account the external heat exchange using the total heat transfer coefficient. External cooling or insulating operations can have an important role on the heat transfer inside the microwave cavity. Steady state conditions, high temperatures, thermal gradients reduc-
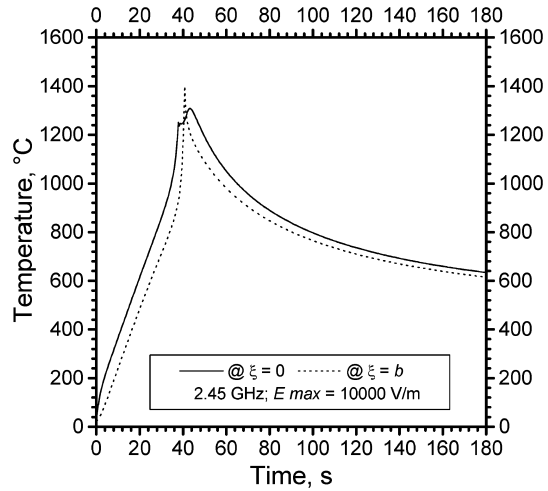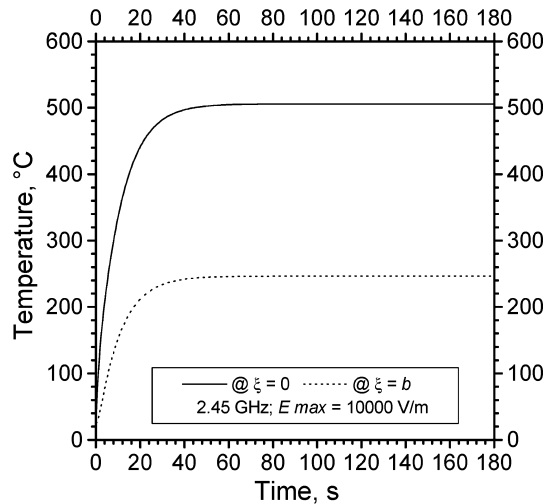
tion are the fundamental effects obtainable modifying the external heat capacity losses.

A semi-quantitative study on the effects of external conditions can be performed simply adopting arbitrary fixed values for the total heat exchange coefficient. In particular, being the heat exchange coefficient in previous section of the order of tenth of $Wm^{-2} K^{-1}$, the external insulation of the cavity has been reproduced imposing low value for h (of the order of several $Wm^{-2} K^{-1}$). Similarly, the presence of an external cooling system has been reproduced by imposing value for total heat exchange coefficient two order of magnitude higher (of the order of hundreds $Wm^{-2} K^{-1}$).

In a rigorous treatise external cooling fluxes or layers of insulating materials must be take in account using appropriated correlations for $h(T)$ and/or introducing an overall heat transfer coefficient in the boundary condition 2.

Figure 14 and 15 report examples of what happens during the microwave heating in presence of the chemical reaction (see the second sub-section), when the total heat

transfer coefficient is changed. Temperature evolutions show the influence on the microwave induced oxidation process when heat transfer coefficient changes (decreases and increases) of one order of magnitude. In particular, in Figure 14 is reported the thermal situation occurring when the total heat transfer coefficient decreases. Due to minor heat losses, chemical reaction reaches more rapidly the ignition point and thermal gradients are very reduced. Vice versa, in correspondence of fast cooling, i.e. high values of h, thermal profiles speedily arrive at the steady states never attaining the ignition points (Figure 15). Under these conditions, the reaction is never supported.

4
Conclusions

Microwave heating processes of weak and of "activated" absorbers are investigated. The significant role of the loss factor is outlined through two crucial aspects: the heating rate and the induced thermal gradients in low conductor materials.

Effects of a chemical reaction assisted by microwave on heat and mass transfer are analyzed. The monitoring of all stages of the chemical reaction performed by thermal and concentration profiles, explained the heat transport and the temperature distribution inner the materials.

Finally, the influence of different external fluid-dynamic conditions on microwave heating processes has been examined. It is shown that external parameters can control heat an mass transfer phenomena during microwave-heating: cold streams or insulating layers applied on the microwave oven can reduce process time and thermal gradients or ensure appropriate thermal profiles in heating treatments.

References

1. Clark DE; Folz DC; West JK (2000) Processing material with microwave energy. Mat Sci Eng A 287: 153–158
2. Zhang H; Datta AK; Taub IA; Doona C (2001) Electromagnetics, heat transfer, and thermokinetics in microwave sterilization. AIChE J 47(9): 1947–1968
3. Thostenson ET; Chou TW (1999) Microwave processing: fundamentals and applications. Composites, Part A: Applied Science and Manufacturing 30: 1055–1071
4. Sutton WH (1989) Microwave processing of ceramic materials. Ceramic Bull 68(2): 376–386
5. Xie Z; Yang J; Huang X; Huang Y (1999) Microwave processing and properties of ceramics with different dielectric loss. J European Ceramic Soc 19: 381–387
6. Haque KE (1999) Microwave energy for mineral treatment processes – a brief review. Int J Miner Process 54: 1–24
7. Kingman SW; Rowson NA (1998) Microwave treatment of minerals – a review. Miner Eng 11(11): 1081–1087
8. Acierno D; Barba AA; d'Amore M (2003) Microwaves in soil remediation from VOC's. 1: Heat and Mass Transfer Aspects (in press). AIChE J
9. Jones DA; Lelyveld SD; Mavrofidis SD; Kingman SW (2002) Microwave heating applications in environmental engineering – a review. Res Conservation Recycling 34: 75–90
10. Metaxas AC; Meredith RJ (1988) Industrial Microwave Heating, London, Peter Peregrinus Ltd
11. Meredith RJ (1998) Engineers' Handbook of industrial microwave heating, London, IEE
12. Chow Ting Chan TV; Reader HC (2000) Understanding microwave heating cavities, Norwood, MA, Artech House Inc
13. Barba AA; Lamberti G (2003) Preliminary validation of a numerical code for heat and mass transfer simulations. Heat Mass Transfer 39(5–6): 429–433
14. Perry RH; Green D (1984) Perry's chemical engineers' Handbook. 7th Edn, Section 5, New York, McGraw-Hill International Editions
15. Lapidus L; Pinder GF (1982) Numerical solution of partial differential equations in science and engineering, New York, John Wiley & Sons
16. Barba AA; Cuccurullo G; d'Amore M (2002) IR temperature measurements in monomode microwave cavity for soot-trap filter regeneration, ThermoSense XXIV, Orlando, FL, SPIE, 4710: 691–698
17. Ciambelli P; Corvo P; Gambino M; Palma V; Vaccaro S (1996) Catalytic combustion of carbon particulate, Catal. Today 27: 99–106
18. Ma J; Fang M; Zhu P; Li B; Lu X; Lau NT (1997) Microwave-assisted catalytic combustion of diesel soot, Appl. Catal. A: General 159: 221–228